Available online at www.sciencedirect.com
SCIENCE DIRECT®
International Journal of Thermal Sciences 42 (2003) 871–880
International Journal of Thermal Sciences
www.elsevier.com/locate/ijts

Local/global analysis applications to ground-coupled heat transfer

Adnan Al-Anzi [a], Moncef Krarti [b,*]

[a] College of Engineering, Department of Architecture, Kuwait University, P.O. Box 5969, Safat, Code No. 13060, Kuwait
[b] CEAE Department, CB 428, University of Colorado, Boulder, CO 80309, USA

Received 27 February 2002; accepted 25 October 2002

Abstract

In this paper, a new local/global analysis technique is developed to solve multi-dimensional ground-coupled heat transfer problems. In particular, the novel method is applied in this paper to determine foundation heat transfer for buildings with slab-on-grade floors. It is found that analytical solutions can be used successfully to capture thermal bridging effect when integrated in the developed local/global analysis technique. In addition, it is found that significant savings in computational effort can be achieved with no sacrifice in accuracy when local/global analysis is used.

1. Introduction

Due to efforts in improving the energy performance of above-grade components of building envelope over the last three decades, the ground-coupled heat transfer contribution to the total energy used in a typical US home has increased significantly. Shipp and Broderick [1] estimated that the heat transfer from an uninsulated foundation in Columbus, Ohio can represent up to 67% of heat loss in a tightly-sealed home that is well insulated above-grade. Globally, earth-contact heat transfer appears to be responsible or 1 to 3 quadrillion KJ in the US [2]. It is estimated that by improving the thermal performance of building foundations, up to 0.5 Quadrillion KJ of annual energy use could be saved in the US [3].

Several insulation configurations for building foundations are currently used. For slab-on-grade floors, it is a common practice to place insulation on either the exterior or interior surface of the foundation wall and/or floor [4]. Fig. 1 shows various slab-on-grade floor insulation placement configurations commonly used in the US. To determine the best insulation configuration for a building foundation, several analysis techniques have been proposed [4]. These analysis techniques can be grouped into two main categories: analytical or numerical techniques. In general, analytical techniques provide useful physical insights but are limited to simplified foundation configurations [5,6]. On the other hand, numerical methods are applied to more realistic foundations configurations but may require large computational efforts [7–9]. A method that combines the advantages of both the analytical and numerical techniques is presented in this paper. In particular, a noval approach based on a local/global analysis technique is developed to solve building foundation heat transfer problems.

Local/global analysis has been used under various forms in the literature for different engineering applications. In particular, local/global analysis is used to increase the efficiency of computational methods for performing stress analysis [10,11]. Specifically, local/global analysis is used to analyze the stress in composite structures using only numerical techniques for both local and global domains. In this paper, the Global analysis is used to determine the thermal behavior within the entire ground/slab domain while the local analysis is used to evaluate the heat transfer in a smaller area located near the slab foundation.

For this new proposed local/global analysis technique, a simplified analytical method is used to develop a solution for the ground-coupled heat transfer problem in the global domain. This global model does not account for the foundation details within the ground/slab domain. For the local domain, a numerical technique is used to find the heat transfer solution within a restricted area within the ground/slab domain that accounts for the foundation details. Foundation details

* Corresponding author.
E-mail address: krarti@bechtel.colorado.edu (M. Krarti).

1290-0729/$ – see front matter
doi:10.1016/S1290-0729(03)00059-0

Nomenclature

a	half width of the slab-on-grade floor	m	
b	water table depth	m	
c	interior perimeter insulation location, shown in Fig. 1	m	
d	height of the above-grade wall	m	
E	far Field distance	m	
e, f	parameters to define the local domain	m	
h	convection heat transfer coefficient	$W{\cdot}m^{-2}{\cdot}K^{-1}$	
k_{conc}	thermal conductivity of the concrete slab floor	$W{\cdot}m^{-1}{\cdot}K^{-1}$	
k_i	thermal conductivity of the insulation layer	$W{\cdot}m^{-1}{\cdot}K^{-1}$	
k_{ss}	thermal conductivity of the ground	$W{\cdot}m^{-1}{\cdot}K^{-1}$	
N	number of terms in a Fourier series		
Q_L	total slab heat loss estimated using the local solution	$W{\cdot}m^{-1}$	
T	temperature	K	
T_a	ambient (indoor or outdoor) air temperature	K	
T_o	outside air temperature	K	
T_i	building indoor air temperature	K	
T_{ss}	slab/soil surface temperature defined by Eq. (4)	K	
w_{fw}	thickness of the foundation footing wall	m	
w_i	thickness of the insulation layer	m	
w_s	thickness of the concrete slab floor	m	
w_{wl}	thickness of the above-grade wall	m	
x, y	space coordinates	m	

Greek symbols

ε_n, δ_n	eigenvalues defined in Eqs. (3) and (4)

Subscripts

i	edge of the slab
iw	inner wall surface
m	middle of the slab
o	outdoor or soil surface
ow	outer wall surface

such as foundation wall can be easily modeled using numerical solution such as Finite Difference Method (FDM). The combined analytical/numerical solution (local/global solution) is compared to a detailed numerical solution using finite difference technique. This study shows that even though simplified analytical solutions fail to account for thermal bridging effects in slab foundations, they are very useful when considered as global solutions for the proposed novel local/global analysis, especially when large domains are considered.

2. General L–G procedure

The new local/global (or simply L–G) analysis technique can be applied to any heat transfer problem. In this paper, the L–G analysis technique is used to determine the ground-coupled heat transfer problems for slab-on-grade floors. Even though steady-state and two-dimensional analysis is considered, the L–G technique can be extended to deal with transient and three-dimensional heat flows for myriad of ground-coupled foundations including basements, crawlspaces, and underground buildings.

The general procedure for the L–G analysis technique proposed in this paper consists of the following steps:

- Define a simplified formulation for the ground-coupled heat transfer problem so it can be solved by an analytical technique such as the ITPE method. For the case of slab foundation, Fig. 2(a) presents one possible global domain (which consists of only the soil domain).
- Solve the ground-coupled heat transfer problem in the global domain using the ITPE technique (or any other analytical technique).
- Define a portion of the global domain that includes the details of the foundation (such as the foundation wall, and slab/wall joint). This portion of the global domain is referred to as a local domain. For the slab foundations, Fig. 2(b) presents one alternative of the local domain.
- Solve the ground-coupled heat transfer in the local domain using a numerical method such as a finite difference method. The temperature profiles at the boundaries of the local domain are those obtained from the analytical solution obtained for the global domain.

Using this L–G analysis, the impact of the foundation details is captured without significant computational effort since the numerical solution is needed only in a small domain (i.e., the local domain).

2.1. Application to slab-on grade floor foundation

Fig. 2 shows the slab foundation model considered in this paper to demonstrate the L–G analysis technique. Fig. 2(a) shows a simplified slab model for the global analysis. In particular, the global slab model ignores the foundation details and the thicknesses of slab floor as well as of the insulation layer and any floor covering. Fig. 2(b) illustrates a more realistic slab model that accounts for all the foundation details including footing wall, slab floor, and insulation layer.

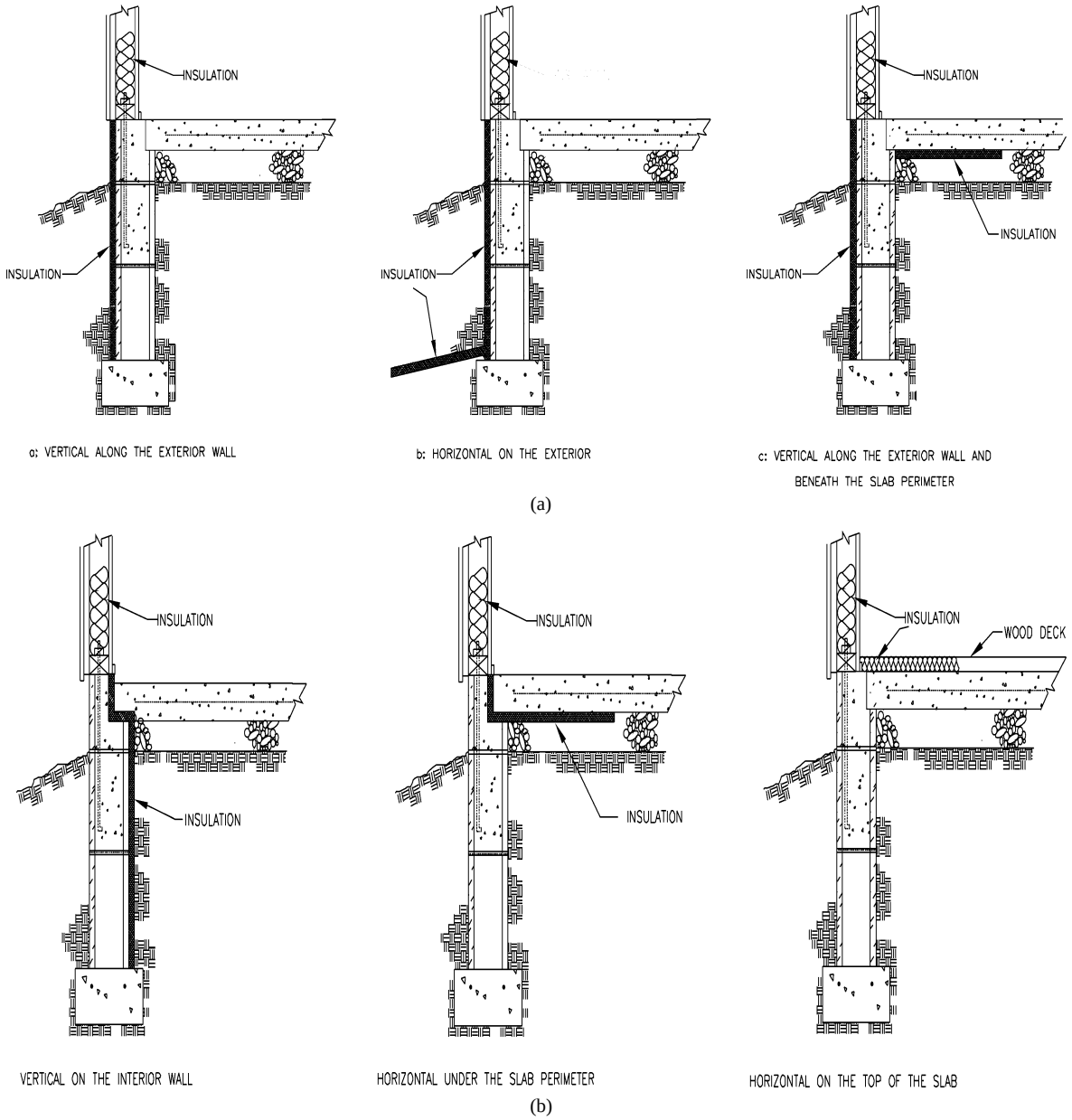

Fig. 1. Common insulation configurations for slab-on-grade floors: (a) exterior placements, and (b) interior placements.

Under steady-state conditions, the temperature distribution within the ground medium and any foundation element, $T(x, y)$ is subject to the Laplace equation:

$$\frac{\partial(k \cdot \frac{\partial T}{\partial x})}{\partial x} + \frac{\partial(k \cdot \frac{\partial T}{\partial y})}{\partial y} = 0 \tag{1}$$

where k is the thermal conductivity of the slab, insulation, or soil medium.

To determine the ground-coupled heat transfer for the slab foundation of Fig. 2, Eq. (1) is first solved. The following boundary conditions are considered:

- Slab and soil surfaces ($y = 0$):

$$k \cdot \frac{\partial T}{\partial x} = h(T_a - T) \tag{1a}$$

where, T_a is the ambient air temperature (either inside or outside the building).

- Water table surface ($y = b$): for this problem, the water table is assumed to be sufficiently deep so that its temperature can be considered constant:

$$T(x, b) = T_w \tag{1b}$$

Experimental studies [4] have shown that water tables can be modeled as isothermal surfaces for depths greater than 5 m (17 ft).

- Symmetry line ($x = 0$) is modeled as an adiabatic boundary condition:

$$\frac{\partial T}{\partial x}(0, y) = 0 \tag{1c}$$

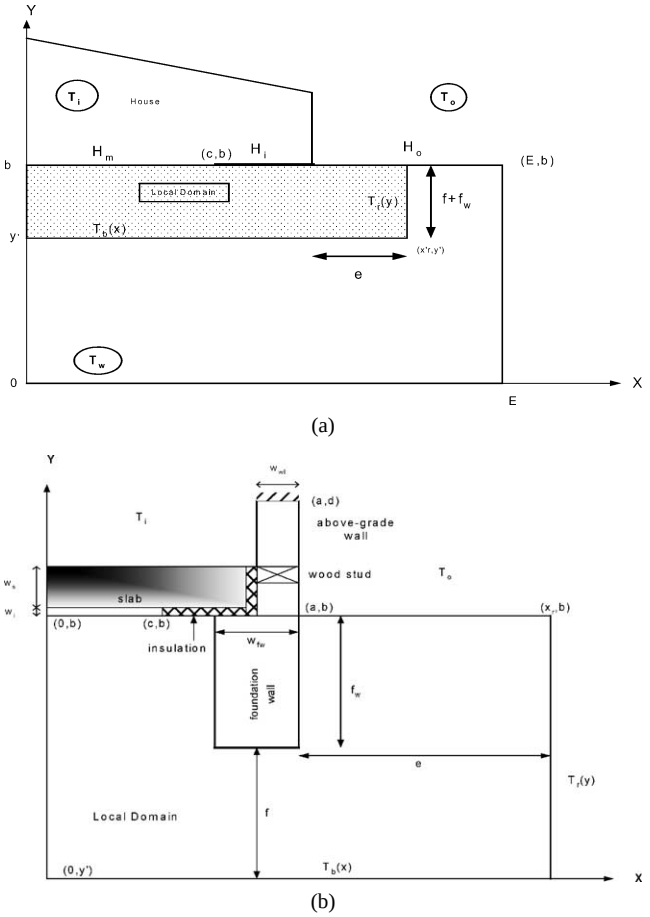

Fig. 2. Local/global model for the slab-on-grade floor foundation with smaller local domain: (a) global model, (b) local model.

- Far field boundary condition ($x = E$), beyond which the building foundation does not affect the soil medium:

$$\frac{\partial T}{\partial x}(E, y) = 0 \tag{1d}$$

- Above-grade wall boundary conditions including:
  At the inner surface of the wall:

$$k_{\mathrm{iw}}\frac{\partial T}{\partial x}(a - w_{\mathrm{wl}}, y) = h_{\mathrm{iw}}\big[T(a - w_{\mathrm{wl}}, y) - T_{\mathrm{i}}\big] \tag{1e}$$

  At the outer surface of the wall:

$$k_{\mathrm{ow}}\frac{\partial T}{\partial x}(a, y) = h_{\mathrm{ow}}\big[T(a, y) - T_{\mathrm{o}}\big] \tag{1f}$$

  At the upper surface of the wall:

$$\frac{\partial T}{\partial y}(x, d) = 0 \tag{1g}$$

The variables used in Eqs. (1a)–(1g) are illustrated in Fig. 2 and are defined in the nomenclature.

2.2. Global solution

Fig. 2(b) illustrates one of several options for a local domain for the slab-on-grade foundation problem considered in this analysis. The soil temperature within the global domain is first obtained using an analytical solution to a simplfied heat transfer problem for the slab foundation. The ground medium in Fig. 2(a) is modeled as an isotropic soil to simplify the mathematical solution and to better illustrate the L–G analysis presented in this paper. The same L–G procedure can be easily applied when nonhomogenous ground such as a layered soil is considered. In the local domain, the foundation details are either ignored (floor and insulation thicknesses and above-grade walls) or are assumed to be as integral parts of the soil medium (foundation walls).

To obtain an analytical solution for the ground-coupled heat transfer problem beneath the slab in the global domain as stated by Eq. (1), an effective convection heat transfer coefficient, h, is defined for Eq. (1a) to represent the equivalent conductance of the slab floor/soil surface including any insulation layer. This heat transfer coefficient can be expressed as follow:

$$h = \begin{cases} h_{\mathrm{m}} & 0 \leqslant x \leqslant c \\ h_{\mathrm{i}} & c \leqslant x \leqslant a \\ h_{\mathrm{o}} & x > a \end{cases} \tag{2}$$

The temperature distribution within the ground (i.e., global domain) can be obtained using an analytical solution technique such as the Interzone Temperature Profile Estimation (ITPE) method [12]. In particular, the temperature profiles $T_{\mathrm{b}}(x)$ and $T_{\mathrm{r}}(y)$ can be expressed by Eqs. (3) and (4), respectively:

$$T_{\mathrm{b}}(x) = \frac{2}{L}\sum_{n=1}^{+\infty} A_n \cos\delta_n x \frac{\sinh\delta_n y_b}{\sinh\delta_n b} - \frac{2}{b}T_{\mathrm{ss}}\sum_{n=1}^{+\infty}\frac{(-1)^n\varepsilon_n}{\varepsilon_n^2}\sin\varepsilon_n y_{\mathrm{b}}\frac{\cosh\varepsilon_n x}{\cosh\varepsilon_n c} \quad x \in [0, x_{\mathrm{r}}] \tag{3}$$

and

$$T_{\mathrm{r}}(x) = \frac{2}{L}\sum_{n=1}^{+\infty} A_n \cos\delta_n x_{\mathrm{r}} \frac{\sinh\delta_n y}{\sinh\delta_n b} - \frac{2}{b}T_{\mathrm{ss}}\sum_{n=1}^{+\infty}\frac{(-1)^n\varepsilon_n}{\varepsilon_n^2}\sin\varepsilon_n y\frac{\cosh\varepsilon_n x_{\mathrm{r}}}{\cosh\varepsilon_n c} \quad y \in [y_{\mathrm{b}}, b] \tag{4}$$

where

$$y_{\mathrm{b}} = b - f$$

$$x_{\mathrm{r}} = a + e$$

$$T_{\mathrm{ss}} = \frac{h_0}{h_0 + k_{\mathrm{ss}}\delta\coth\delta b}$$

$$\delta_n = \frac{(2n-1)\pi}{2L}$$

$$\varepsilon_n = \frac{n\pi}{b}$$

$$A_n = \int_0^L A(x)\cos\delta_n x\,\mathrm{d}x$$

The temperature profiles $T_b(x)$ and $T_r(y)$, provided by respectively Eqs. (3) and (4), are set as new boundary conditions for the local domain as shown in Fig. 2(b).

2.3. Local solution

The local domain consists of the area represented by Fig. 2(b) includes the foundation details consisting of actual floor and insulation thicknesses as well as the floor/wall joints. The local domain is defined by soil/slab surface and two boundaries which are characterized by the temperature $T_b(x)$ at $y = y_b$ and $T_r(y)$ at $x = x_r$.

The temperature variation in the local domain, $T_L(x, y)$, subject to Eq. (1) with the boundary conditions of Eqs. (1a) through (1f), is solved numerically using a finite difference technique based on a non-uniform discretization scheme and an expansive mesh. The total slab heat loss/gain is solved numerically by integrating the temperature gradient temperature along the slab surface $[0, a]$:

$$Q_L = 2\int_0^a h_i\big[T_i - T_L(x,b)\big]\,\mathrm{d}x \tag{5}$$

where h_i is the convective heat transfer coefficient at the inner surface of the floor slab and $T_L(x, b)$ is the floor surface temperature obtained from the local solution.

In this paper, the benefits of the L–G analysis compared to purely numerical methods are investigated. In addition, effects of the local domain size on the accuracy of the solution are discussed.

3. Discussion of the results

In this section, the soil medium shown in Fig. 2(a) is considered as the global domain for a building slab foundation. The analytical solution of the ground-coupled heat transfer within the global domain is based on the Fourier series presented by Eqs. (2) and (3). In order to perform the calculations, the sum in the Fourier series has to be truncated to N terms. The effect of the truncation number N on the accuracy of the analytical solution is first investigated. The effect of the local domain size on the accuracy of the L–G solution is then discussed.

The slab-on-grade floor foundation used to generate the results shown in this paper has the following characteristics:

- Concrete slab: half width, $a = 5.0$ m (16.4 ft); thickness, $w_s = 0.10$ m (0.33 ft); concrete thermal conductivity, $k_{conc} = 1.731$ W·m^{-1}·K^{-1} (1.01 Btu/hr.ft.F);
- Insulation layer: thickness, $w_i = 0.05$ m (0.16 ft); uniform insulation, $c = 0$; insulation thermal conductivity, $k_i = 0.0275$ W·m^{-1}·K^{-1} (0.016 Btu/hr.ft.F);
- Footing wall: thickness, $w_{fw} = 0.15$ m (0.5 ft); depth, $f_w = 1.0$ m (3.28 ft);
- Above-grade wall: thickness, $w_{wl} = 0.11$ m (0.37 ft); height, $d = 1.5$ m (4.92 ft);
- Water table: depth $b = 5.0$ m (16.4 ft); temperature, $T_w = 10\,^\circ$C (50 F);
- Indoor temperature $T_r = 20\,^\circ$C (68 F);
- Outdoor temperature $T_o = 15\,^\circ$C (59 F);
- Soil thermal conductivity $k_{ss} = 1.2$W·m^{-1}·K^{-1} (0.70 Btu/hr.ft.F);
- Far field distance: $E = 17$ m (55.7 ft).

3.1. Accuracy of the global solution

The accuracy of the global solution is a function of the number of truncation, N, used to compute the sums in the Fourier series of the analytical solution. Obviously, the higher the value of N, the better is the accuracy but the higher is the required computational effort.

Fig. 3 shows the variation of the normalized total slab heat loss and the CPU time as a function of the truncation number, N. Two slab insulation configurations are considered in the analysis presented in Fig. 3 (uninsulated slab and R-10 (i.e., R-value = 1.76 m$^2\cdot{}^\circ$C^{-1}·W^{-1}) uniformly insulated slab). Fig. 3 clearly indicates that the analytical solution provides good estimation of total slab heat loss/gain for $N = 25$ with relatively little computational effort. The relative percent error for the total slab heat loss obtained with $N = 100$ is less than 0.15% from that obtained with $N = 1000$ for both uninsulated and uniformly insulated slab configurations as indicated in Fig. 3. Meanwhile, the CPU time required for a truncation of $N = 100$ is 8.19 seconds using an AMD K6-200 MHz processor, which is almost 30 times less than that for a truncation of $N = 1000$ (for which the CPU time is 225 seconds using the same AMD k6-200 MHz processor).

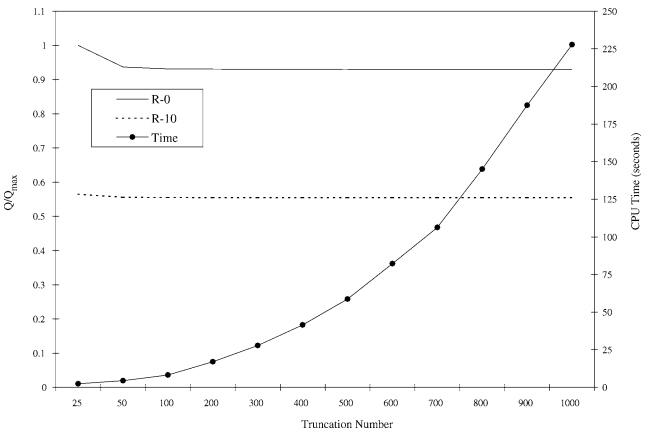

Fig. 3. Effect of the truncation number N on the calculation accuracy of the global solution for the total slab heat loss and the CPU time where $Q_{max} = 18.12$ W·m^{-1}.

3.2. Accuracy of the local model

Two parameters, e and f, are used to define the size of the local domain as indicated in Fig. 2(b). The extension, f, represents the depth below the bottom of the foundation wall of the local domain lower boundary. The larger the value of f, the closer the lower boundary of the local domain is to the water table defined as an isothermal boundary condition. Meanwhile, the extension, e, is the distance between the foundation wall exterior surface and the right boundary of the local domain. Therefore, the parameter, e, indicates how close the local domain is to the slab foundation surface.

Fig. 4 shows the effect of increasing the values of both parameters, e and f, on the total slab heat loss as calculated by the L–G solution. For comparison purposes, the accuracy of the L–G solution is determined relative to the detailed numerical solution. It should be noted that the detailed numerical solution is obtained when the local domain coincides with the global domain. Fig. 4 presents the accuracy of the L–G solution for two slab insulation configurations (an uninsulated slab for Fig. 4(a) and R-10 (RSI-1.76) uniformly insulated slab for Fig. 4(b)) using the same slab characteristics used in Fig. 2.

For the case of the uninsulated slab shown in Fig. 4(a), the percent difference between the L–G solution and the numerical solution—to calculate the total slab heat loss/gain—reduces as the ratio f/b increases. Even when $f/b = 0.1$, the difference between the L–G solution and the numerical solution is only 1.35%. The effect of the parameter e on the accuracy of the L–G solution is less significant than that of the parameter, f. In particular, the percent difference between the L–G analysis and the detailed numerical solution remains unchanged for $e/E > 0.3$. This result indicates that without any significant loss of accuracy, the local domain

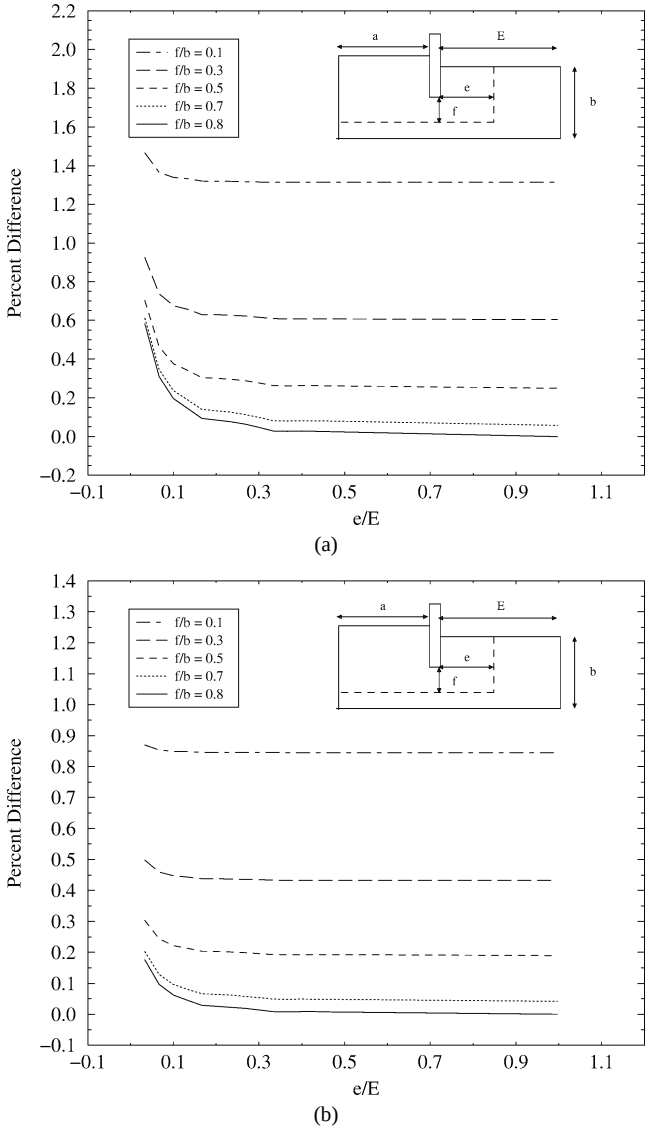

Fig. 4. Effect of the parameters e and f on the accuracy of the local/global solution for (a) uninsulated slab; (b) R-10 (RSI-1.76) uniformly insulated slab.

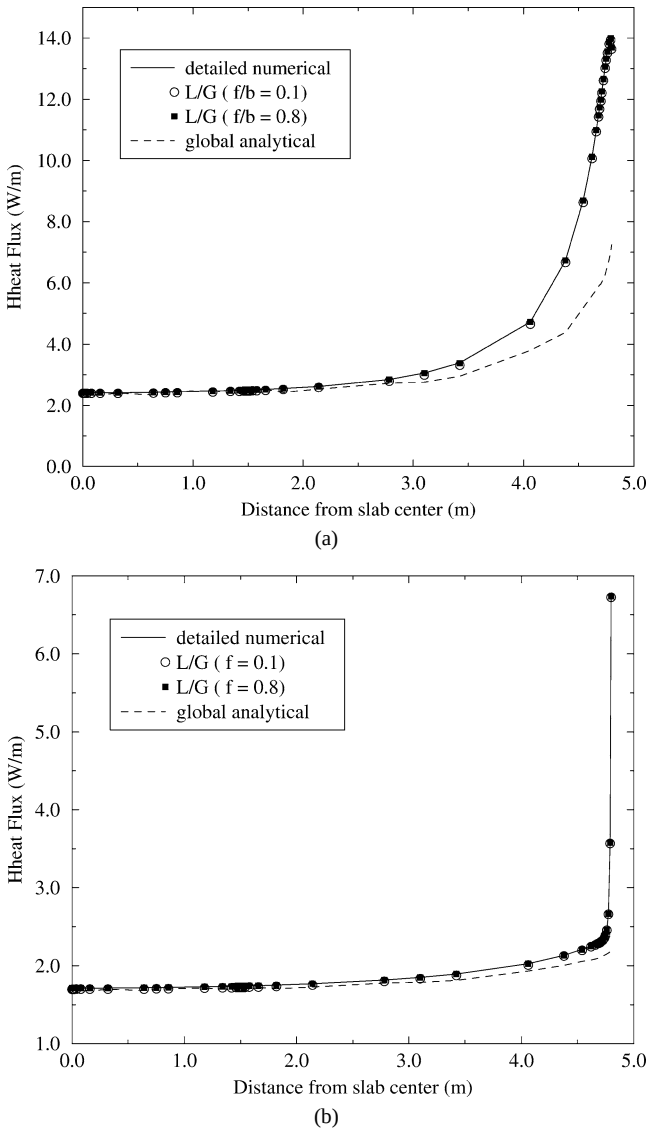

Fig. 5. Heat flux distribution for various f values for: (a) uninsulated slab, and (b) R-10 (RSI-1.76) uniformly insulated slab.

can be made smaller by reducing the value of e (in the horizontal direction) rather than f (in the vertical direction).

Fig. 4(b) illustrates the effect of the parameters, e and f, on the accuracy of the L–G solution for R-10 (RSI-1.76) uniformly insulated slab. In general, similar results to those found for the uninsulated slab (see Fig. 4(a)) are obtained for the insulated slab case, with the exception that even smaller percent differences relative to the detailed numerical solution are achieved using the L–G analysis. Indeed, the accuracy of the L–G solution is about 0.85% at $f/b = 0.1$, and 0.45% at $f/b = 0.3$. It should be noted that the percent difference between the detailed numerical and L–G solutions is the same at high f/b values whether the slab is insulated or not.

Fig. 5 shows the heat flux distribution for various values of the parameter, f. The difference between the heat flux distribution results for $f/b = 0.1$ (i.e., with a small local domain) and $f/b = 0.8$ (i.e., with relatively large local domain) is minimal. As expected, the heat flux distribution for $f/b = 0.8$ is closer to that obtained from the detailed numerical solution (which corresponds to the case of $f/b = 1.0$).

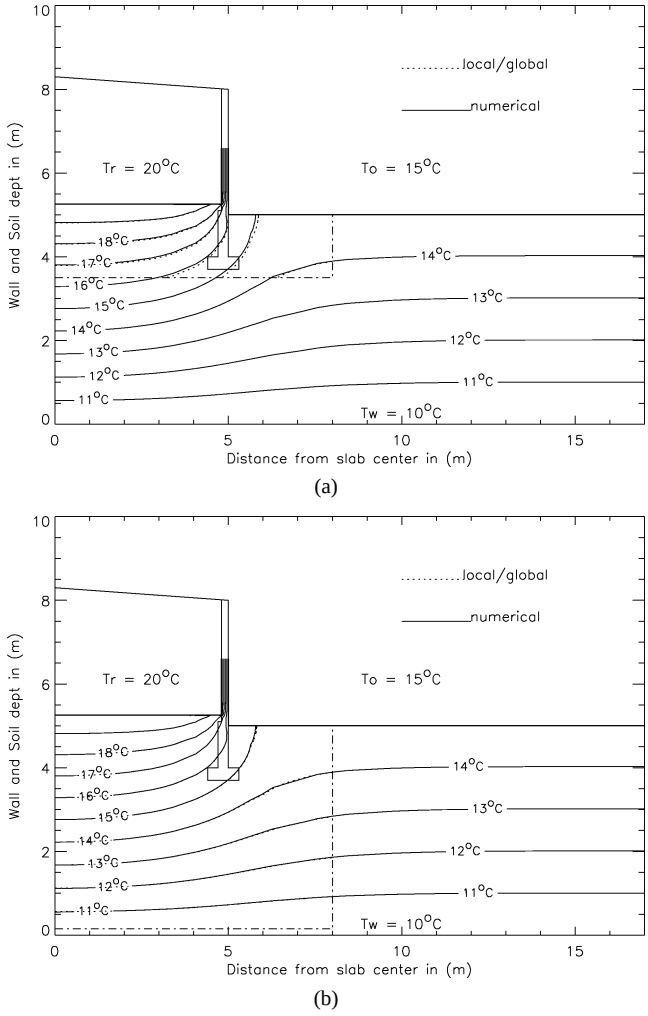

Fig. 6. Temperature distribution for uninsulated slab for: (a) $f/b = 0.1$, and (b) $f/b = 0.8$.

Moreover, Fig. 5 clearly indicates that the simplified global analytical solution fails to capture the heat transfer behavior at the slab/wall joint, where thermal bridging occurs. However, the inaccuracy of the simplified global analytical solution is reduced for a slab with higher insulation levels as shown in Fig. 5(b).

Fig. 6 presents the temperature distribution within the ground and the foundation elements for an uninsulated slab with $f/b = 0.1$ (Fig. 6(a)), and $f/b = 0.8$ (Fig. 6(b)). The agreement between the L–G solution (dashed line) and the detailed numerical solution (solid line) is slightly better for $f/b = 0.8$ (i.e., larger local domain) as shown in Fig. 6(b). It is clear from the results of Fig. 6 that the global analytical solution gives good predictions of ground temperatures in areas not close to the foundation details.

When insulation is added to the slab, the comparative results indicate that the difference between the L–G solution and the detailed numerical solution is even smaller than that obtained for uninsulated slabs. Therefore, smaller local domains can be used for insulated slabs.

3.3. Effect of soil thermal conductivity

This section investigates the effect of soil thermal conductivity on the accuracy of the L–G solution, compared to the detailed numerical solution, to estimate total slab heat loss.

Fig. 7(a) shows the percent difference in predicting total slab heat loss between the L–G solution and the detailed numerical solution for an uninsulated slab as a function of the soil thermal conductivity, k_{ss}. When $f/b = 0.1$, the percent difference is minimum and is less than 0.6% for $k_{ss} = 0.3$ W·m^{-1}·K^{-1} (2.1 Btu/hr.ft.F). However, the percent difference increases with soil thermal conductivity and reaches a maximum value when $k_{ss} = 1.2$ W·m^{-1}·K^{-1} (8.3 Btu/hr.ft.F). Thereafter, the percent difference reduces as the soil conductivity increases. The reason for this behavior is the thermal bridging effects (i.e., multi-dimensional heat transfer) associated with the foundation details. The foundation thermal bridging effects are modeled by the local solution, but are not captured by the global solution for low values of f/b (i.e., small local domain). For low values of soil thermal conductivity, the soil acts as an insulator, and this reduces the thermal bridging effects attributed to the foundation raised floor and wall/floor joint. For very high values of soil thermal conductivity, the concrete in the foundation details acts as an insulator causing the thermal bridging effect to be smaller. For an intermediate value of soil thermal conductivity ($k_{ss} = 1.2$ W·m^{-1}·K^{-1} (8.3 Btu/hr.ft.F)), the thermal bridging effects are significant and are not well accounted for by an L–G solution obtained with a small local domain.

Fig. 7(b) provides the percent difference in predicting total slab heat loss between the L–G solution and the detailed numerical solution for R-10 (RSI-1.76) uniformly insulated slab. The existence of insulation in both local and

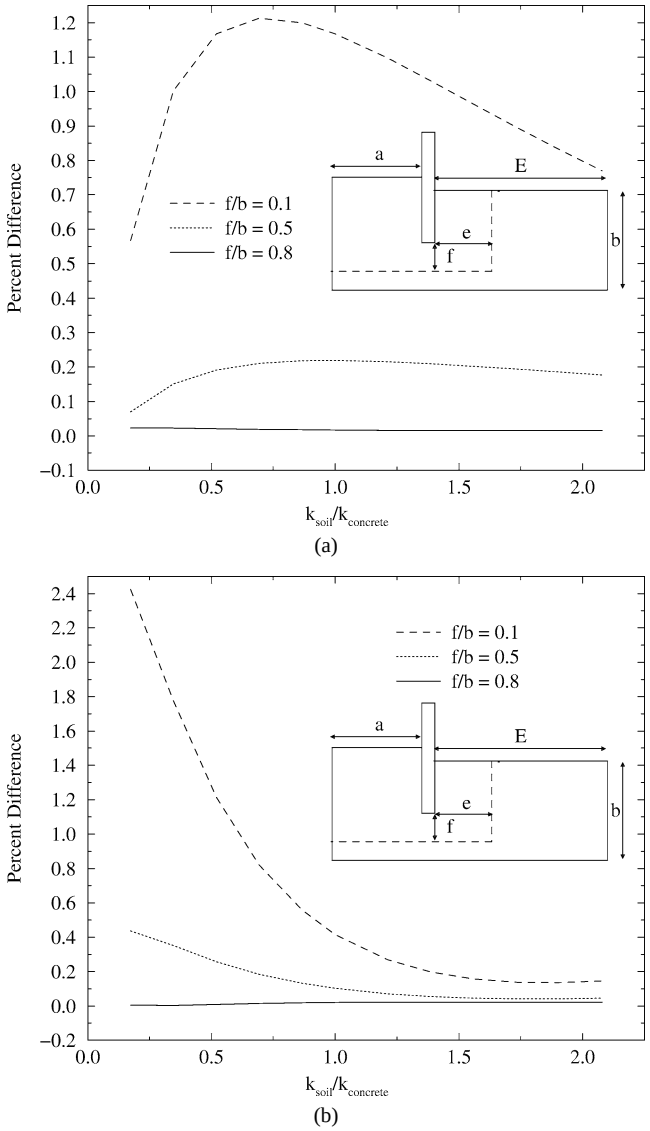

Fig. 7. Effect of soil thermal conductivity on the accuracy of local/global solution (the percent difference in total slab heat loss between the local/global solution and the detailed numerical solution) for: (a) uninsulated slab, and (b) R-10 (RSI-1.76) uniformly insulated slab.

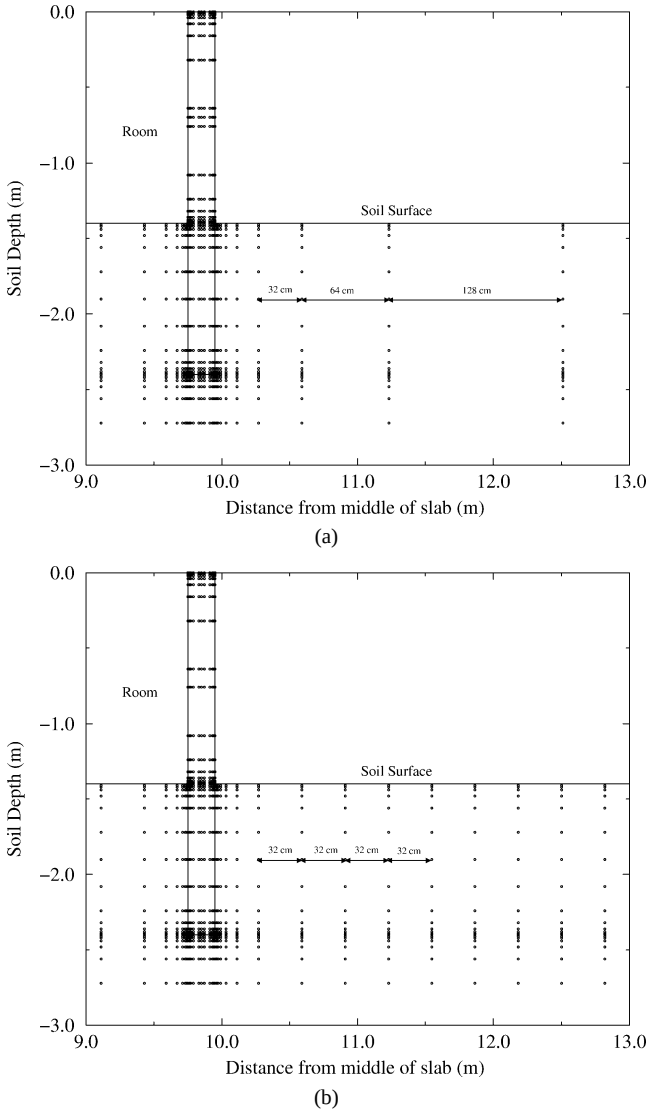

Fig. 8. Mesh generation schemes used in the local solutions with: (a) free expansive mesh, and (b) restricted expansive mesh.

global models reduces the thermal bridging effects caused by the foundation details. However, these effects reach an asymptotic value as the soil thermal conductivity, k_{ss}, increases. Moreover, the percent difference between the L–G and the detailed numerical solutions decreases as f/b values increase. For small local domains (i.e., f/b less than 0.5) the accuracy of the L–G solution improves as the soil thermal conductivity increases.

3.4. Effect of discretization scheme for the local solution

The local solutions for all the cases of L–G solutions considered so far in this paper are determined using a free expansive mesh. A free expansive mesh is a mesh that expands freely throughout the solution domain. A restricted expansive mesh has a small discretization scheme and can be considered as an alternative to improve the accuracy of the local solution without considerable computational efforts. Basically, the restricted expansive mesh is refined in only selected sections of the solution domain and uses a rough and uniform mesh in the remaining domain. In particular, the descritization mesh is fine in areas where there is a sudden change in material thermal properties or a sudden change of temperature conditions. The restricted expansive mesh is a suitable discretization scheme especially for large slabs, where free expansive mesh may not provide the desirable accuracy level. Fig. 8 illustrates both a restricted expansive mesh and the free expansive mesh for a typical slab foundation model.

Fig. 9(a) presents the percent difference between predictions obtained from L–G solution and detailed numerical solution for various mesh discretization schemes and local domain sizes. The results in Fig. 9(a) are generated for the case where the slab half width $a = 5.0$ m. It is clear that restricted

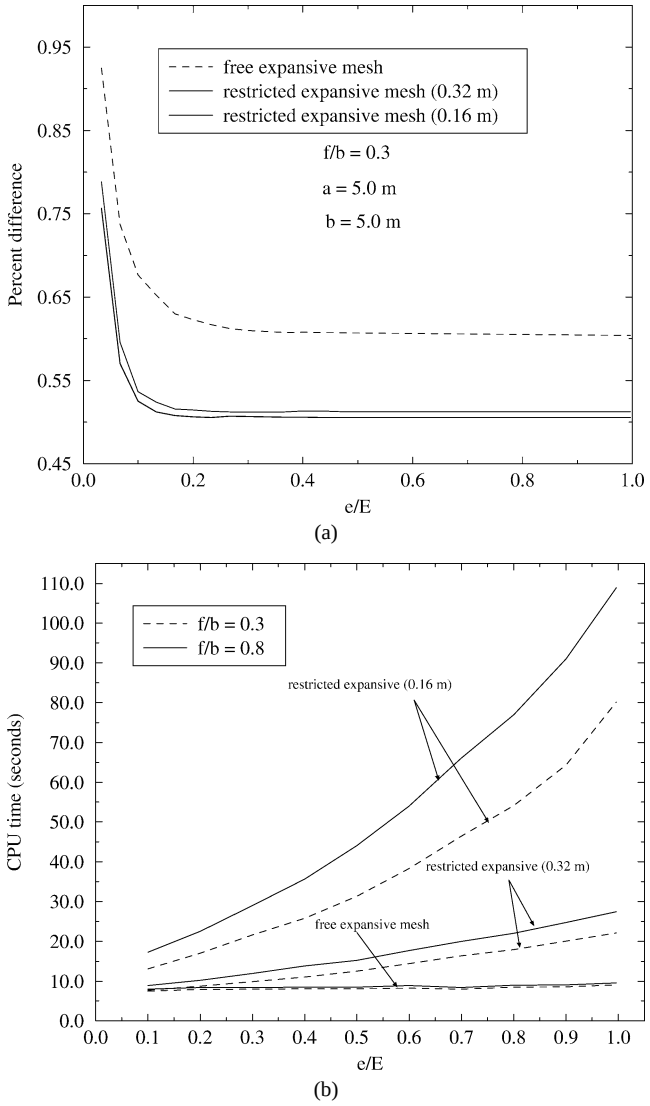

Fig. 9. Effect of mesh generation scheme on: (a) the accuracy, and (b) the CPU time of the local/global solution for an uninsulated slab.

expansive mesh gives better accuracy for the L–G solution than the free expansive mesh. In fact, the percent difference for the free expansive mesh solution is larger than 0.6% for $e/E > 0.3$, while, for the restricted expansive mesh, it is less than 0.5% for the same case. In addition, Fig. 9 indicates that reducing the uniform part in the restricted expansive mesh does not significantly improve the solution. For example, reducing the space increment from 0.32 m to 0.16 m improves the solution by less than 0.01%.

Fig. 9(b) presents the computational efforts expressed in CPU time required to obtain L–G solutions using different mesh generation schemes. It is clear that restricted expansive mesh requires more CPU time than free expansive mesh. For instance, it takes 8.06 s to run a L–G solution with the expansive mesh, 12.51 s with a restricted expansive mesh of 0.32 m space refinement, and 31.27 s with a restricted expansive mesh of 0.16 m space refinement for $e/E = 0.5$ and $f/b = 0.3$. The CPU time required to obtain

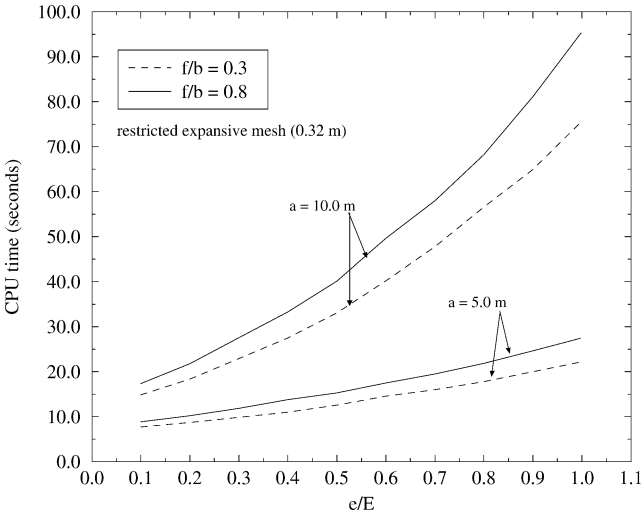

Fig. 10. Effect of large slabs on the CPU time to generate local/global solutions.

the numerical solution are respectively 10.00 s for the free expansive mesh, 30.00 s for the restricted expansive mesh with space refinement of 0.32 m, and 110.00 s for the restricted expansive mesh with space refinement of 0.16 m. Meanwhile, the global solution (i.e., the analytical solution) takes a CPU time of less than 8.19 s to generate using $N = 100$.

As a reminder, the CPU time statistics presented above are specific to a slab with a half width $a = 5.0$ m and to an AMD K6 200 MHZ processor. These results indicate that no significant reduction in computational efforts can be obtained with the free expansive mesh, but 31% of CPU time can be saved when restricted expansive mesh of 0.32 m space refinement is used. In addition, 64% of CPU time is saved when restricted expansive mesh of 0.16 m space refinement is used. The CPU time savings can be even more significant when large global domains are considered (as it will be illustrated in the next section), or when 3-D analysis is performed.

3.5. *Effect of slab size on CPU time*

A comparative analysis of the CPU time requirements to obtain the L–G solutions for slabs with half widths of $a = 5.0$ m and $a = 10.0$ m is shown in Fig. 10. The results indicate a considerable increase in the computational efforts is required when the slab half width increases from $a = 5.0$ m to $a = 10.0$ m. For instance, it takes 33.09 seconds to obtain a L–G solution for $a = 10.0$ m with $e/E = 0.5$, while it takes only 12.59 seconds for $a = 5.0$ m with $e/E = 0.5$. Thus, it takes about 2.5 time more computational effort to solve the ground-coupling problem for building foundations with a half width $a = 10$ m than that required for slabs with a half width $a = 5$ m. Applications of L–G analysis to large slabs are therefore more promising regarding CPU time savings.

Using finite difference techniques, three-dimensional solutions for slab-on-grade floor foundations require typically several hours to estimate annual ground-coupled heat transfer [9]. Based on analytical techniques, solutions for steady-periodic three-dimensional simplified slab models can be obtained in few seconds [13]. Thus, the L–G analysis technique is expected to offer substantial reductions in computing time to solve transient three-dimensional ground-coupled problems when compared to purely numerical methods. These reductions in execution time would make building foundation models based on the L–G analysis technique more suitable than numerical models for integration with whole-building simulation programs.

4. Summary and conclusions

It has been shown that the advantages of analytical and numerical techniques can be combined using a new local/global (L–G) analysis approach to determine the thermal performance of building foundations. The L–G analysis uses an analytical solution to solve the heat transfer problem within the global domain. A numerical technique is then considered to obtain the heat transfer solution for the local model which includes all the foundation details that are ignored by the global model.

Excellent agreement of less than 2.5% is obtained for all cases analyzed in this paper between the L–G analysis and a detailed numerical solution which is applied to the entire slab/soil domain including foundation details. Based on the results presented in this paper, the local domain can be made sufficiently small as long as it includes all the foundation details not accounted for in the global domain. In addition, it was found that the proposed L–G analysis can save significant CPU time for large slabs and/or where fine discretization grid are used.

The new L–G analysis is particularly useful in evaluating the effects of various design parameters of a slab foundation with minimal computational efforts. An application of the proposed L–G analysis is to determine the thermal bridging effects of slab/wall joint on total foundation heat transfer [14]. Moreover, the L–G analysis technique can be extended to deal efficiently with transient three-dimensional analysis of building foundations.

References

[1] P.H. Shipp, T.B. Broderick, Analysis and, comparison of annual heating loads for various basement wall insulation strategies using transient and steady-state models, in: F.A. Govan, D.M. Greason, J.D. McAllister (Eds.), Thermal Insulation, Materials, and Systems for Energy Conservation in the 80's, in: ASTM STP, Vol. 789, American Society for Testing and Materials, 1983.

[2] D. Claridge, Design methods for earth-contact heat transfer, in: K. Boer (Ed.), Progress in Solar Energy, American Solar Energy Society, Boulder, CO, 1988.

[3] K. Labs, J. Carmody, R. Sterling, L. Shen, Y. Huang, D. Parker, Building Foundation Design Handbook, ORNL Report Sub/86-72143/1, Oak Ridge, TN, Oak Ridge National Laboratory, 1988.

[4] M. Krarti, Foundation heat transfer, in: Y. Goswami, K. Boer (Eds.), Advance in Solar Energy, Vol. 13, American Solar Energy Society, Boulder, CO, 2000.

[5] K. Landman, A. Delsante, Steady-state heat losses from building floor slab with horizontal edge insulation, Building Environ. 22 (1) (1987) 57–60.

[6] C. Hagentoft, Heat losses and temperature in the ground under a building with and without ground water flow—I. Infinite ground water flow rate, Building Environ. 31 (1) (1996) 3–11.

[7] G.P. Mitalas, Calculation of basement heat loss, ASHRAE Trans. 89 (1983), Part 1B.

[8] P.H. Shipp, Basement, crawlspace, and slab-on-grade thermal performance, Proceedings for Thermal Performance of Exterior Envelopes of Buildings II, 1983.

[9] W.P. Bahnfleth, C.O. Pedersen, Three-dimensional modelling of heat transfer from slab floors, ASHRAE Trans. 96 (1990), Part 2.

[10] R. Ballarini, Local–global analysis of crack growth in continuously reinforced ceramic matrix composites, Report for National Aeronautics and Space Administration, 1989.

[11] J.D. Whitecomb, K. Woo, Application of iterative global/local finite-element analysis, Part 2: Geometrically non-linear analysis, Comm. Appl. Numer. Methods 24 (1993) 757–766.

[12] M. Krarti, D. Claridge, J.F. Kreider, The ITPE technique applied to steady-state ground-coupling problems, Internat. J. Heat Mass Transfer 31 (1988) 1885–1898.

[13] P. Chuangchid, M. Krarti, Steady-periodic three-dimensional foundation heat transfer from refrigerated structures, ASME J. Solar Energy Engrg. 122 (2000) 69–83.

[14] A. Al-Anzi, M. Krarti, Evaluation of the magnitude of thermal bridges of slab-on-grade floor foundations, in: Proceedings of Solar 2000: Solar Powers Life, Share the Energy, June 16–21, Madison WI, USA, 2000, pp. 470–482.